Chapter 9
Experimental Investigation of Spray Characteristics of Kerosene, Ethanol, and Ethanol-Blended Kerosene Using a Gas Turbine Hybrid Atomizer

**Amlan Garai, Shinjan Ghosh, Swarnendu Sen
and Achintya Mukhopadhyay**

Abstract Gas turbines have wide applications as prime movers in transportation and power-generating sectors, most of which are currently driven by fossil fuels. The problem of air pollution can be associated with the use of conventional fuels, and their prolonged use has caused the fuel reserves to get depleted gradually. The addition of ethanol in conventional fossil fuel leads to better spraying characteristics and decreases air pollution as well. The present work is done for knowing the spray characteristics of pure kerosene, pure ethanol, and ethanol-blended kerosene (10 and 20% ethanol-blended kerosene by volume) by using a hybrid atomizer. The novelty of the hybrid atomizer lies in the fact that the fuel stream is sandwiched between two annular air streams. Tangential inlets are used for both fuel and air stream; however, the inner air stream can be used in axial configuration. A high swirling effect is produced outside the nozzle due to the tangential inlet of the flow direction. The direction of the fuel flow and both the air streams in the atomizer may be configured in the same direction or in opposite directions, respectively. The inner and outer air flow rates are varied continuously. Here, backlight imaging technique is used for capturing the spray images. Various spray breakup regimes like distorted pencil, onion, tulip, and fully developed spray regimes have been observed. The breakup length, cone angle, and sheet width of the fuel stream are analyzed from the images for different fuels and air flow rates. It is observed that

A. Garai (✉) · S. Sen · A. Mukhopadhyay
Department of Mechanical Engineering, Jadavpur University, Kolkata 700032, India
e-mail: amlangarai@gmail.com

S. Sen
e-mail: sen.swarnendu@gmail.com

A. Mukhopadhyay
e-mail: achintya.mukho@gmail.com

S. Ghosh
Department of Mechanical and Aerospace Engineering, University of Central Florida,
Orlando, FL 32826, USA
e-mail: shinjandgp025@gmail.com

breakup length decreases for ethanol-blended kerosene due to low viscosity of ethanol. It is also observed that at higher air flow rate, breakup length decreases due to turbulent nature of the fuel stream.

9.1 Introduction

The rapid depletion in the fossil fuel reserves and the emission of greenhouse gases from vehicle exhausts are pressing issues for the global environment. There has been an upsurge in the environmental pollution since the last century which in turn has led to global warming and erratic climatic changes. To prevent further damage to the environment, researchers have been trying to develop alternative fuel technologies with low exhaust emission. In this regard, ethanol may be treated as an appropriate alternative, due to its lower viscosity and low combustion emission. The use of ethanol blended with diesel was a subject of research in the 1980s, and it was shown that ethanol–diesel blends were technically acceptable for existing diesel engines (Hansen et al. 2005). Ethanol can be produced from crops with high sugar or starch contents. Some of these crops are sugarcane, sorghum, corn, barley, cassava, sugar beets, etc. Ethanol can be identified as one of the feasible alternative fuels (Yahya and Goering 1977). This type of research work was started from 1970s. Gasohol (a mixture of 10% alcohol with 90% gasoline) is now a commercial
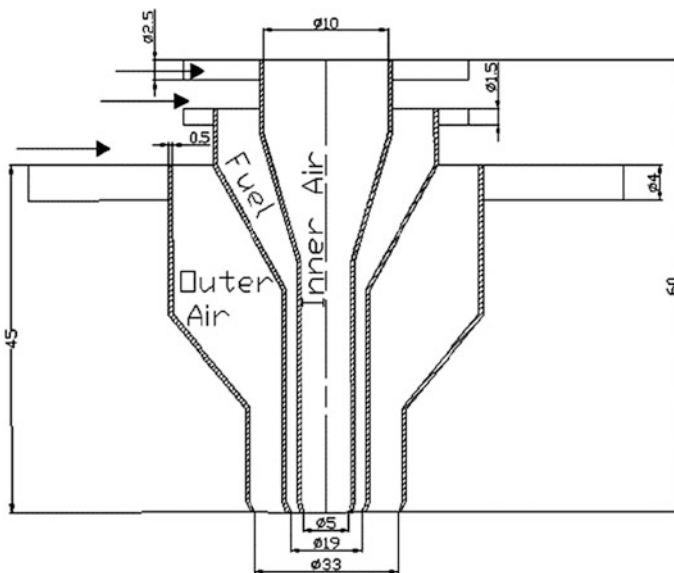

Fig. 9.1 Cross-sectional view of the atomizer all dimension in mm (Chatterjee et al. 2015; Garai et al. 2017)

fuel in over 35 countries of the world including the USA, Canada, and France (Ajav and Akingbehin 2002). In Brazil, car engines have been modified for running on neat alcohol (Reeser et al. 1995) .

A few research projects are going on for comparative study on emission characteristics and ethanol-based fuel in diesel engine. The impacts of ethanol on emissions vary with engine operating conditions and ethanol content. At high load operating conditions, ethanol-blended diesel fuels have stronger effects on smoke, NOx, acetaldehyde emissions, and unburned ethanol emissions, but at low loads,
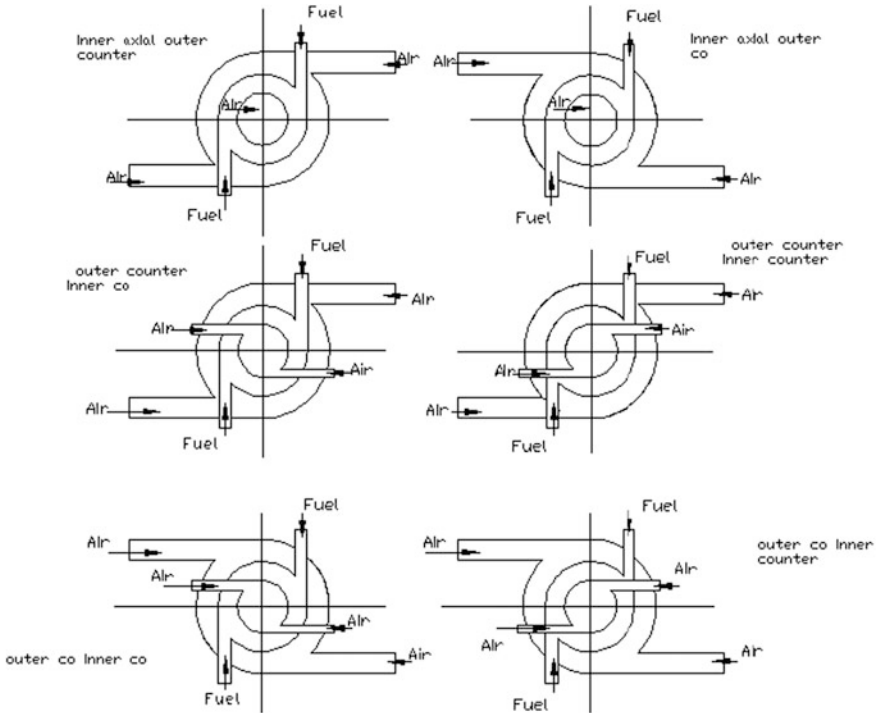

Fig. 9.2 Inlet configuration of the atomizer

Table 9.1 Property of the blended fuel and pure fuel

Particulate	Viscosity (cSt)	Surface tension (dynes/cm)	Calorific value (MJ/Kg)
Kerosene (KE0)	1.38	25.6	46.7
10% ethanol-blended kerosene (KE10)	1.34	25.3	44.2
20% ethanol-blended kerosene (KE20)	1.26	25.1	43.01
Ethanol (KE100)	1.24	24.6	29.5
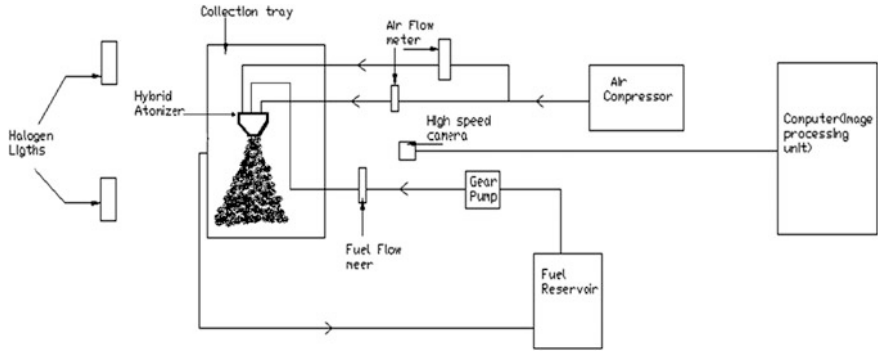
Fig. 9.3 Block diagram of experimental setup

(a) Jet   **(b)** Necklace   **(c)** Onion

(d) Tulip   **(e)** Full Cone   **(f)** Early Breakup
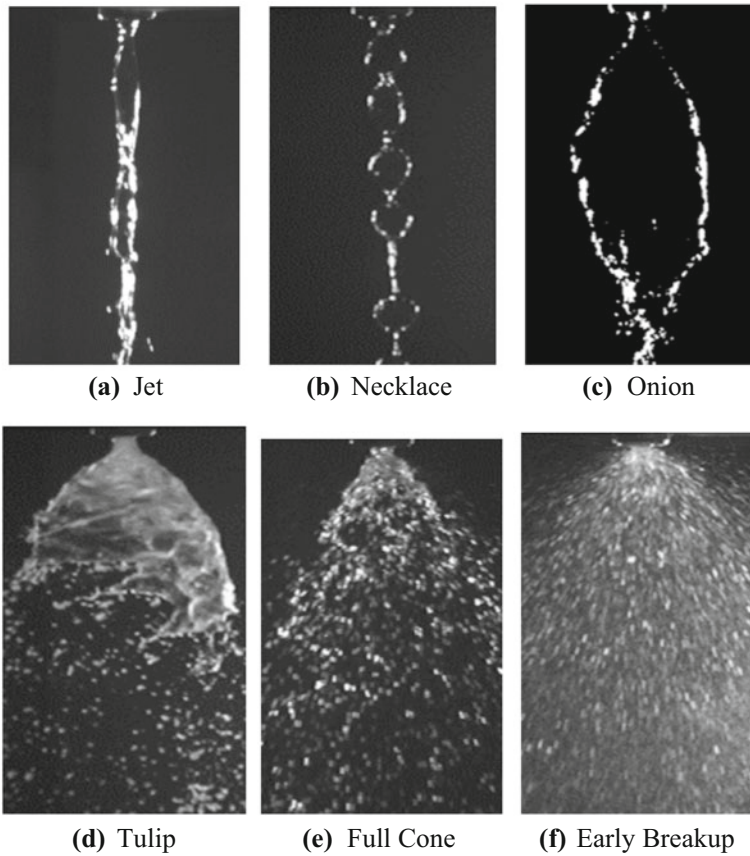
Fig. 9.4 Different breakup stages during spray formation

the blends have slight effects on smoke reduction on a four-cylinder direct injection diesel engine (He et al. 2003). Increasing of ethanol percentage in diesel ethanol blended fuels, DS (dry soot) in the PM (particular matter) and smoke decrease significantly, but the SOF (soluble organic fraction) mass percentage increases above 20% ethanol blended diesel at all lodes (Chen et al. 2007). Xing-Cai et al. (2004) studied about the cetane number improvement additive and also studied the emission and heat release rate on ethanol-blended diesel fuel. Ethanol-blended diesel fuel can be used as a gas turbine fuel.

Khan et al. (2013) studied the thermal efficiency and fuel consumption rates of cooking stove using 5, 10, 15, and 20% ethanol-blended kerosene. Dioha et al. (2012) have also studied the performance of the cooking stove by calculating the boiling time of specified volume of water using different blending of ethanol–kerosene blends. Patra et al. (2015) studied the flame characteristics and combustor performance of the kerosene and kerosene–ethanol blends. They also observed that the soot formation in flame decreases with increasing blend percentage of ethanol. Khalil and Gupta (2013) studied the combustion characteristics of gaseous and liquid fuels for finding an alternative fuel. They used methane, diluted methane, hydrogen-enriched methane, and propane as gaseous fuels and kerosene and

Fig. 9.5 Breakup regimes for developing spray on 1 LPM kerosene flow

ethanol as liquid fuels. They reported that NO and CO emissions were reduced for using the alternative fuels. Without any modifications of the injectors, ethanol-blended kerosene can be used. Pure jet A fuel was blended with ethanol and butanol at varying volume fractions, and performance characteristics along with emission characteristics were studied by Mendez et al. (2012, 2014). They reported that CO and NO_x emissions were reduced for using both types of blended fuels. Lower emissions were also detected in case of fossil fuel blends with four pure vegetable oils in an experiment performed on a 30 KWe commercial micro-gas turbine by Chiariello et al. (2014).

The present study has been concentrated on ethanol-blended diesel and ethanol-blended kerosene fuel. Also, the spray character of blended fuel is compared with the pure fuel. Spray characteristics study has also played a significant role for combustion study. For this study, a hybrid atomizer is used for knowing the inner and outer air flow effects on spray field.

Fig. 9.6 Breakup regimes for developing spray on 2 LPM kerosene flow

9.2 Equipment and Method

9.2.1 Atomizer

The atomizer is a device which is used for discharging a high-velocity liquid into a relatively slow-moving air or gas stream or a low-velocity liquid stream discharge into relatively high-velocity air stream. Major adverbial atomizers are pressure atomizer, simplex atomizer, rotary atomizer, air-assist atomizer, and air-blast atomizer. Different types of nozzles produce three canonical geometrical shapes of liquid: jet, planar sheet, and annular sheet (Lin 2003). Our study is concentrated on a simple gas turbine atomizer spray at low air flow regime. Pressure-swirl atomizers and the air-blast atomizers are commonly used in gas turbine engines. In a pressure-swirl atomizer, a high-pressure liquid discharges into a slow-moving environment. This generally leads to a lot of soot formation. In an air-blast nozzle, liquid is discharged at low velocity into a fast-moving gas (air) flow resulting in a fine spray with good air–fuel mixture. For solving such problems, hybrid atomizers (Chin et al. 1999; Rizk et al. 1996) have been designed that combine the features of
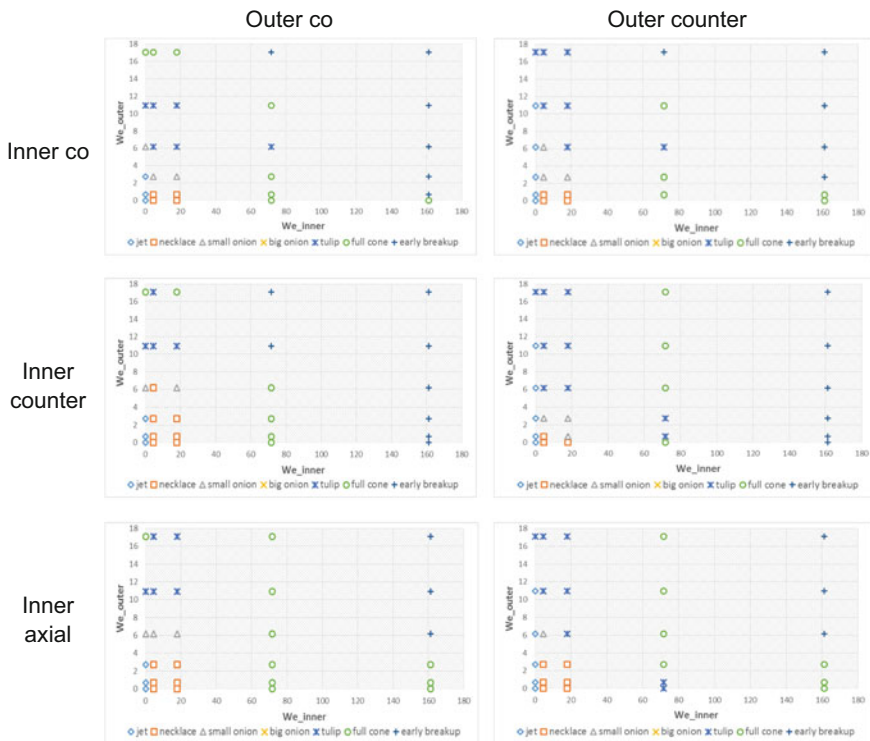

Fig. 9.7 Breakup regimes for developing spray on 1 LPM ethanol flow

both pressure-swirl and air-blast atomizers using the combined effects of air momentum and fuel pressure. Recently, air-blast atomizer is an area of immense interest in industrial and aircraft field due to its reduced emission characteristics and reduced injection pressures. In the present study, a modified hybrid atomizer is used for knowing the effect of inner and outer air at liquid sheet breakup. The different breakup regimes in the spray zone have also been studied. Rizk et al. (1996) and Chin et al. (1999) studied the spray characteristics of a hybrid atomizer, where liquid was flowing into center part of the nozzle and air is flowing into outer periphery of the nozzle. Leboucher et al. (2010) studied the different breakup processes on an annular liquid sheet assisted by coaxial gaseous flow.

In this present study, a hybrid atomizer is used. The hybrid is a combination of pressure-swirl and air-blast atomizers. In this atomizer, annular liquid sheet is sandwiched between two air streams. Tangential inlet ports are used in liquid inlet and outer air and inner air inlets. The tangential inlet is used for producing swirling effect in the spray field. Ma (2002) did an experimental work for studying the effect of tangential inlet on the spray regime. Ibrahim and Jog (2007) studied the nonlinear

Fig. 9.8 Breakup regimes for developing spray on 2 LPM ethanol flow

breakup model for a pressure-swirl atomizer. They also used tangential inlet for producing the swirling effect in the spray regime.

Figure 9.1 Cross–sectional view of the atomizer (all dimension in mm). The dimension of the present nozzle is very much similar with the nozzle used by Chatterjee et al. (2013, 2014, 2015) and Carvalho and Heitor (1998). In the present study, six different configurations are studied by combining the above inlet arrangements (Fig. 9.2). The swirl direction of fuel is kept constant while that of inner and outer air streams are changed. The swirl directions of air streams are either the same as those of the fuel stream (defined as 'co') or opposite to the direction of the fuel sheet (defined as 'counter'). The inner air is also fed in axial direction for one configuration (defined as 'inner axial'). The flow rate of inner air has been varied between 0 and 30 LPM in steps of 10, and the flow rate of fuel stream is 1 and 2 LPM. The variation of spray characteristics with outer air stream flow rate has been studied by varying the outer air flow rate from 0 to 50 LPM in steps of 10. The air flow rate is less than actual gas turbine engine air flow rate. This study has been done for knowing the effect of the spray at low air flow rate. This study was made to understand the atomization effect on the liquid sheet. The flow rates are not sufficient for gas turbine combustion. Figure 9.2 shows the nozzle inlet configuration.

Fig. 9.9 Breakup regimes for developing spray on 1 LPM 10% ethanol-blended kerosene flow

9.2.2 Blend

In the present experiment, the spray atomizer was used to ascertain the characteristics of kerosene, pure ethanol, and two types of ethanol–kerosene blends. For the preparation of the blend, 99.9% concentrated ethanol (manufactured by MARK Germany) was used. During this experimental process, ethanol has been mixed with kerosene at 10 and 20% by volume ratio. The blend has been made at 30 °C by using 2% cosolvent tetrahydrofuran (C_4H_8O) for the 20% blend. When the blend is produced, it is observed that initially, the ethanol is properly mixed up with the kerosene. However, a week later, the blend separates into two layers for the 20% ethanol-blended kerosene fuel. At low temperature, water separation occurs from the blended fuel. The water content of the blended fuel also plays an effective role in phase separation of the blended fuel (Lapuerta et al. 2007; Li et al. 2005).

In order to ascertain the degree of deviation of the blended fuel from the conventional fuel (kerosene in this case), certain properties need to be determined by experimentation such as viscosity, surface tension, and blend stability from the spray and atomization point of view. Ajav and Akingbehin (2002) studied the fuel
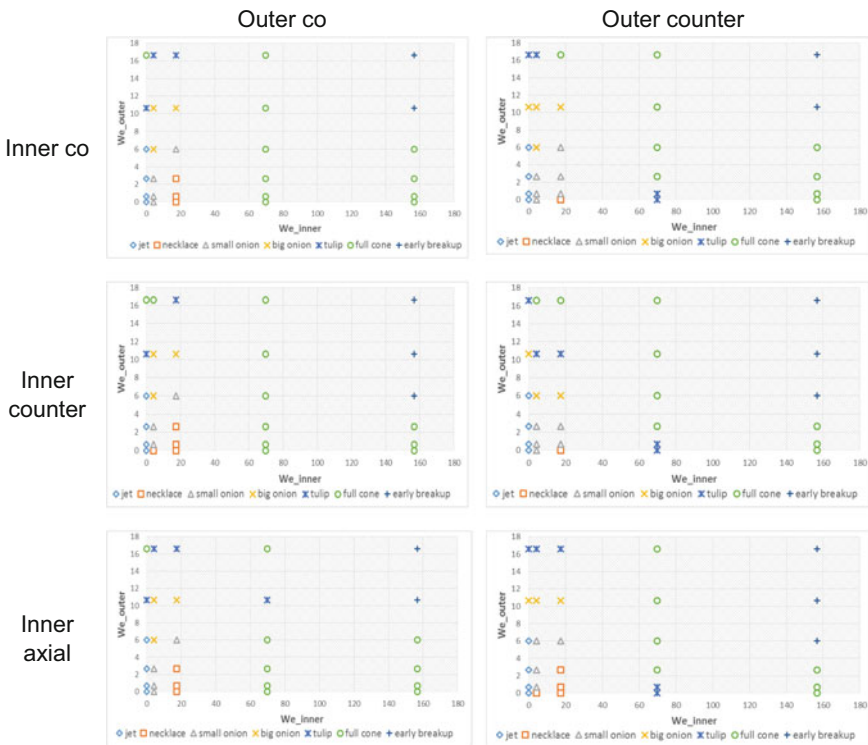

Fig. 9.10 Breakup regimes for developing spray on 2 LPM 10% ethanol-blended kerosene flow

properties like relative density, cloud and pour point, viscosity, and calorific value for 5% to 30% ethanol-blended diesel fuel. They reported that the relative density and viscosity of the blends decreased upon increasing the ethanol percentage in blended fuel. He et al. (2003) also studied the carbon content of the blended fuel and C/H ratio of the ethanol-blended diesel fuel. Brake specific fuel consummation, brake thermal efficiency, and the emission characteristics of the ethanol-blended diesel fuel were studied in a water-cooled single-cylinder direct injection (DI) diesel engine by Li et al. (2005).

In the present study, viscosity, surface tension, and calorific value of the blended fuel and the pure fuel are measured. The Ostwald viscometer (also known as U-tube viscometer or capillary viscometer) (Vesztergom 2014), the du Noüy ring tensiometer, and the bomb calorimeter (Parr, model-6100) are used for measuring the viscosity, surface tension, and calorific values, respectively, for all types of fuel at room temperature. Table 9.1 shows the measured values of the aforesaid fuel properties for pure and blended fuels. It can be observed that all three properties for kerosene are slightly higher than those of the blended fuels and ethanol. It can be seen that calorific value of ethanol is very low compared to that of the other fuels
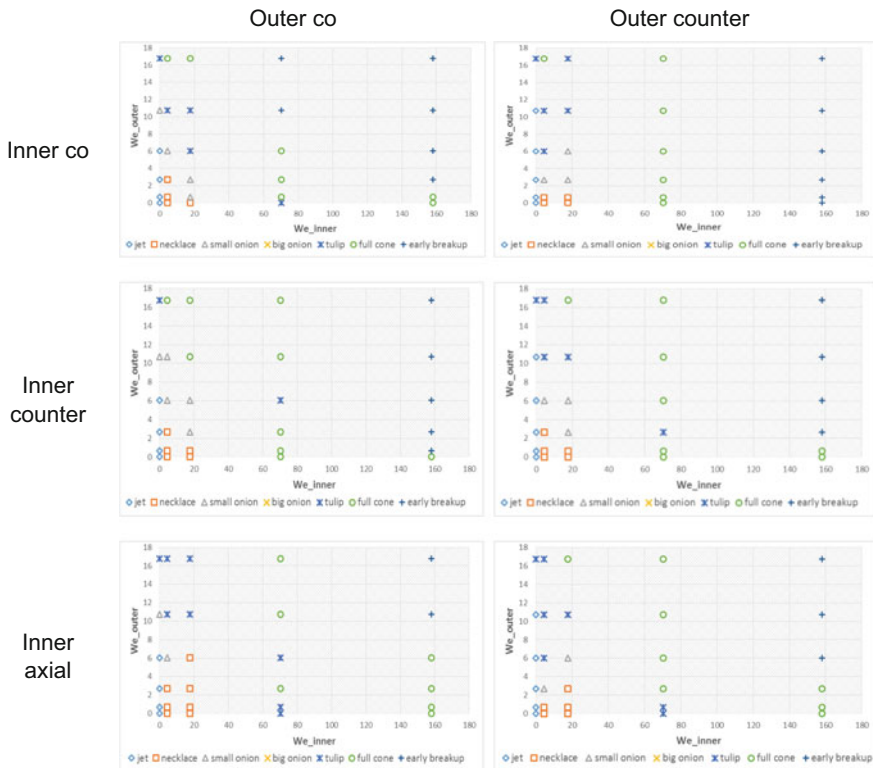

Fig. 9.11 Breakup regimes for developing spray on 1 LPM 20% ethanol-blended kerosene flow

which make it an unsuitable candidate. Sayin (2010) reported that for the lower viscosity, alcohol can be atomized easily in air, producing less emission for its high stoichiometric air–fuel ratio, high oxygen content, and low sulfur content. Drop size decreases with increasing air/liquid mass ratio and air velocity and increases with the increasing liquid viscosity and surface tension (Carvalho and Heitor 1998).

9.2.3 Experimental Setup and Image Capturing Technique

A variety of image capturing techniques can be used for capturing the spray image. For example, Wahono et al. (2008) used two types of image capturing techniques. One was volume lighting mode, and another was backlighting mode. For volume lighting technique, four sets of halogen lights (total power of 4 kW) were used to provide volume illumination of the spray. And for backlighting technique, a halogen light (2 kW) was placed directly behind the spray. Duke et al. (2010) used a photographic measurement technique by using a backlit arrangement illuminating the focal plane of the camera optics in which the liquid sheet is placed.

**Fig. 9.12** Breakup regimes for developing spray on 2 LPM 20% ethanol-blended kerosene flow

For this present study, the backlit imaging technique is used with two halogen lights (1 KW each) for illumining the spray field. The position and angle of the light are optimized for best image contrast. A high-speed camera (Prosilica high-speed camera, 230 fps, model—CV1280, digital machine vision camera, 1280 × 1024 monochrome, 1394 DCAM) is used for capturing the spray images (Fig. 9.3).

The fuel is fed from a gear pump (manufactured by Rotodyne pump and system Ahmedabad (India), 1440 rpm, MAX. DISP. Vol. = 20 LPM and driven by single phase 50 Hz 370 W 4.4 A ½ HP motor), and both air streams are fed from a compressor (manufactured by ELGI Equipment Ltd., model—SA OF 01 080 OF, DISP. Vol. = 92 LP and driven by a single phase, 1 HP, 1450 rpm AC motor.). Rotameters (0–4 LPM kerosene rotameter is used after calibrating with used fuel for measuring the different fuels' flow rates and air rotameter 0–50 LPM used for measuring the air flow rate) are used in all fluid inlet lines for flow rate measurement.

9.3 Results and Discussion

The present study is done with the aid of a hybrid atomizer. This atomizer is a combination of air-blast atomizer and a pressure-swirl atomizer. In a simplex-type pressure-swirl atomizer, an air-cored vortex is formed within the swirling liquid. This air core plays a major role in producing a hollow cone spray (Lefebvre 1989).

Fig. 9.13 Macroscopic spray characteristics (SW = sheet width, L_b = breakup length, θ = cone angle)
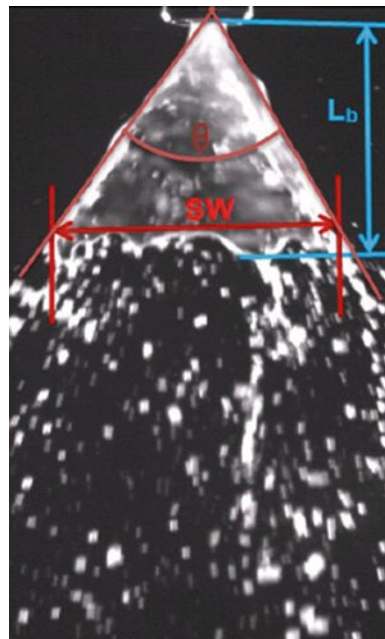
In the present study, the annular liquid sheet is sandwiched between two swirling and inner axial air streams. The annular liquid sheet also has a swirling velocity. The relative magnitude of the tangential and axial components of the swirling velocity at the nozzle outlet plays a significant role in the development of the spray cone angle. For the present experiment, liquid flow is maintained at 1 and 2 LPM flow rate. Outer air flow rate is maintained on 0, 5, 10, 20, 30 LPM, and inner air flow rate is maintained on 0–50 LPM with 10 LPM interval.

For understanding the effect of surface tension on the air–liquid interface at different breakup stages, we calculate the Weber number for inner air (**We_inner**) and outer air (**We_outer**) as follows:

$$\text{We\_inner} = \frac{\rho v^2 l_i}{\sigma} \qquad (9.1)$$
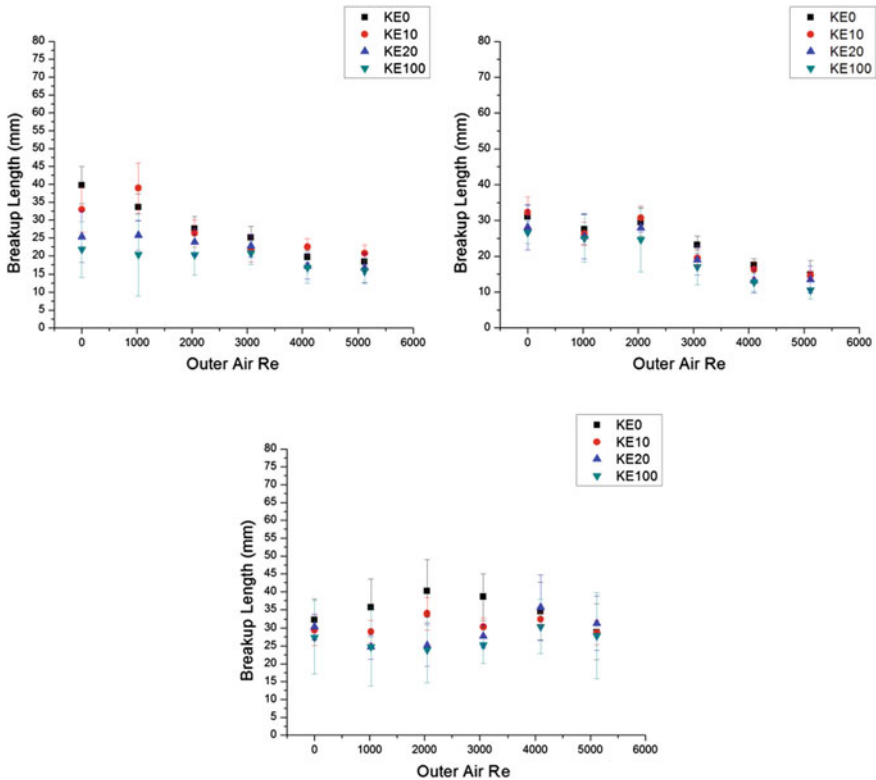

Fig. 9.14 Breakup length variation for different blended fuels with increasing inner air for outer co-swirl configuration and inner co-swirl (upper left), inner counter-swirl (upper right), and inner axial (below) configurations at 1 LPM fuel flow rate

$$\textbf{We\_outer} = \frac{\rho v^2 l_o}{\sigma} \qquad (9.2)$$

In order to measure the macroscopic spray characteristics like breakup length, cone angle, and sheet width, we calculate the Reynolds number (**Re_outer**) for outer air flow as follows:

$$\textbf{Re\_outer} = \frac{\rho v l_o}{\mu} \qquad (9.3)$$

Here, ρ is the density of air, v is the velocity of the air, σ is the surface tension of the fuel–air interface, μ is the viscosity of the air, l_i is the characteristic length of the inner part of the nozzle (taken as inner diameter), and l_o is the characteristic length of the outer part of the nozzle (taken as outer diameter of the nozzle).
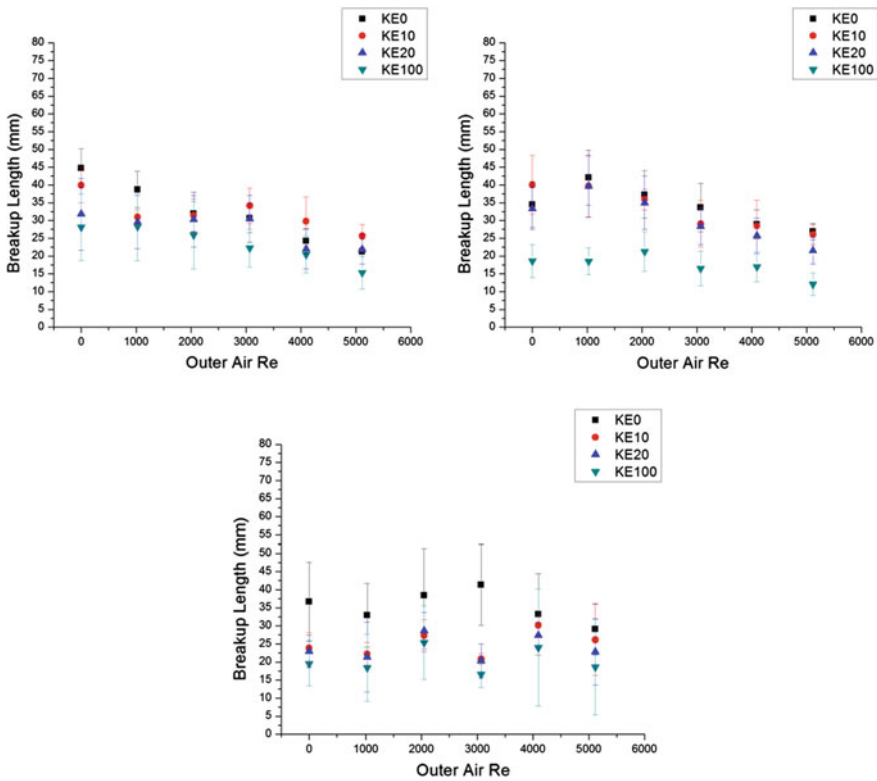

Fig. 9.15 Breakup length variation for different blended fuels with increasing inner air for outer counter-swirl configuration and inner co-swirl (upper left), inner counter-swirl (upper right), and inner axial (below) configurations at 1 LPM fuel flow rate

9.3.1 Breakup Phases

Different breakup regimes are found during the spray development. The relative magnitudes of various velocity components play a vital role in producing the different breakup regimes. These breakup regimes are mainly jet, necklace, onion, tulip, full cone, and early breakup regime. Most preferable breakup regimes are fuel cone and early breakup regimes. Lefebvre reported that these spray stages are formed due to the injection pressure of the liquid (Lefebvre 1989). Figure 9.4 shows the different breakup stages during spray formation.

The liquid sheet which emanates without any major perturbations on the liquid outer surface is called the jet-type liquid sheet as shown in Fig. 9.4a. The nozzle outer air region is stationary, and liquid flow rate is low without any inner air flow. This type of liquid sheet travels a long distance, and the breakup length is very high. The liquid inlet pressure is low, and the nozzle inlet–outlet pressure difference is
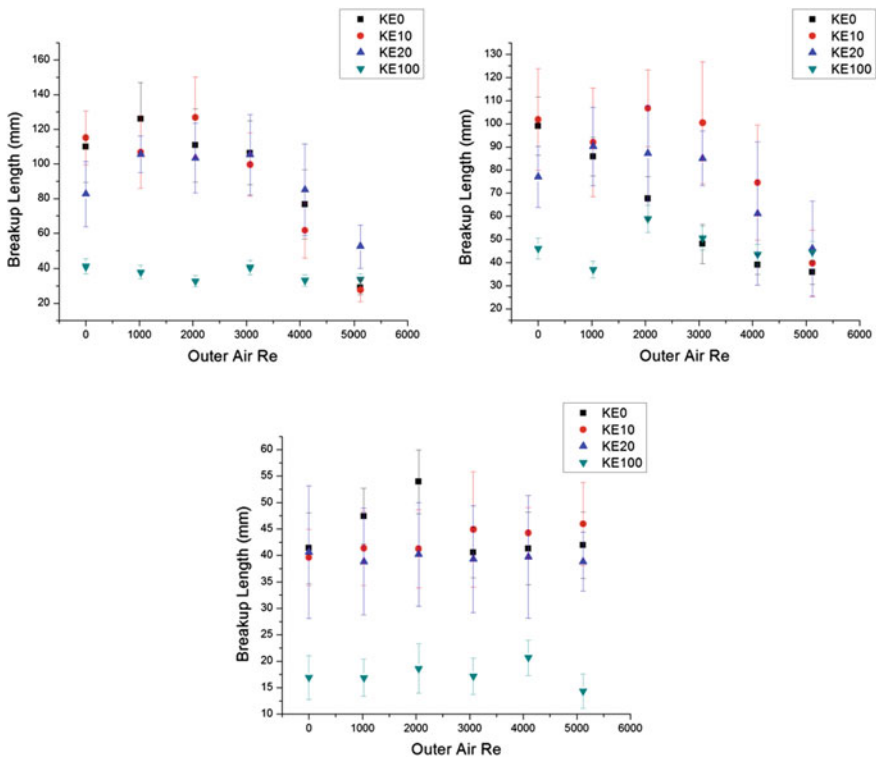

Fig. 9.16 Breakup length variation for different blended fuels with increasing inner air for outer co-swirl configuration and inner co-swirl (upper left), inner counter-swirl (upper right), and inner axial (below) configurations at 2 LPM fuel flow rate

low. The liquid sheet instability growth rate is also very low. The instability is primarily caused by the outer air.

The necklace-type spray shape as shown in Fig. 9.4b is normally formed in situations of low pressure difference between nozzle inlet and nozzle outlet. At very low inner air flow rate, the inner air gets entrapped between the annular liquid sheets resulting in the formation of this shape. Also at very low outer air flow, the outer air creates a low-pressure regime outside the annular liquid sheets creating instability in the outer surface of the annular liquid sheet. For the counter-swirling inner flow, the opposite directions of swirls on the two sides of the liquid sheet lead to modulation of the sheet along the axial direction. This gives rise to a necklace-like structure, particularly at low inner air flow rates and moderate outer air flow rates. Similar structure has also been observed by Zhao et al. (2015). However, in their configuration, there was no outer air flow. Necklace formation is favorable for better spray characteristics.

The onion-type shape as shown in Fig. 9.4c is also formed due to low pressure difference between nozzle inlet and nozzle outlet but the pressure difference in this
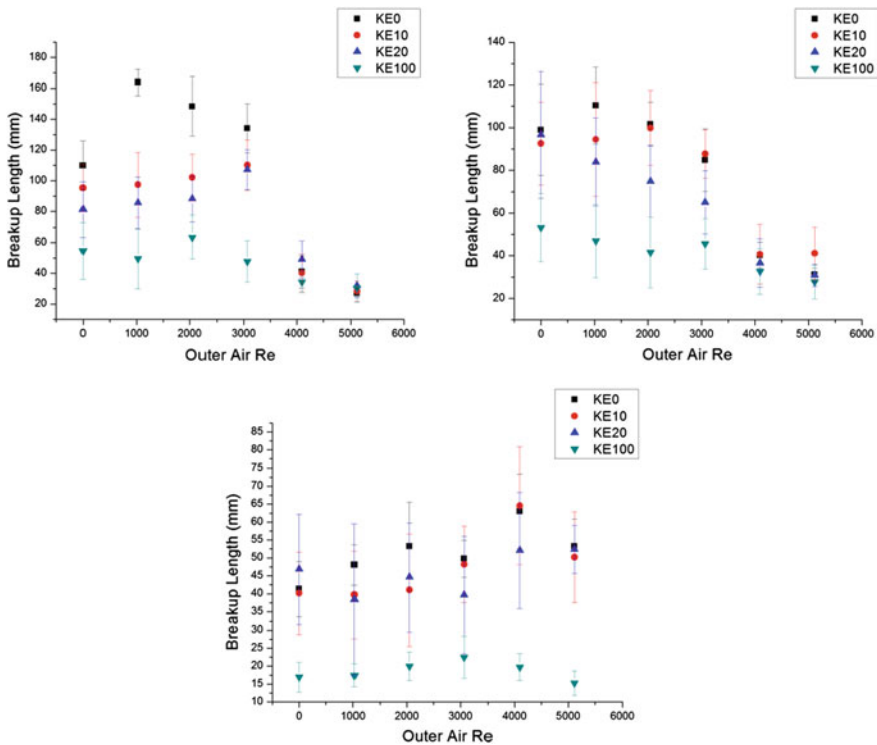

Fig. 9.17 Breakup length variation for different blended fuels with increasing inner air for outer counter-swirl configuration and inner co-swirl (upper left), inner counter-swirl (upper right), and inner axial (below) configurations at 2 LPM fuel flow rate

case is higher than that in case of the necklace-like shape. In the present study, the inner and outer air flow rates are higher than the necklace-type inner and outer air flow rates. The high outer flow creates a low-pressure regime outside the spray regime, which causes the annular liquid sheet to form a bulge of the jet. The swirl direction plays an important role in the formation of big and small bulges. The outer air flow rate also plays a crucial role here. From the spray snapshots, we observe that the inner co-swirl and counter-swirl configurations have higher breakup lengths at lower flow rates due to the formation of a stable onion structure. A slight bulge of the jet is observed at low inner and outer air flow rates. A bigger bulge is created as the outer flow rate increases, and the higher strength of the outer swirling flow induces greater tangential momentum to the annular liquid sheet. This can be observed at the onset of the onion structure formation. Onion shape is usually observed in pressure-swirl atomizers, where the swirling liquid sheet surrounds an air core whose velocity is not so high.
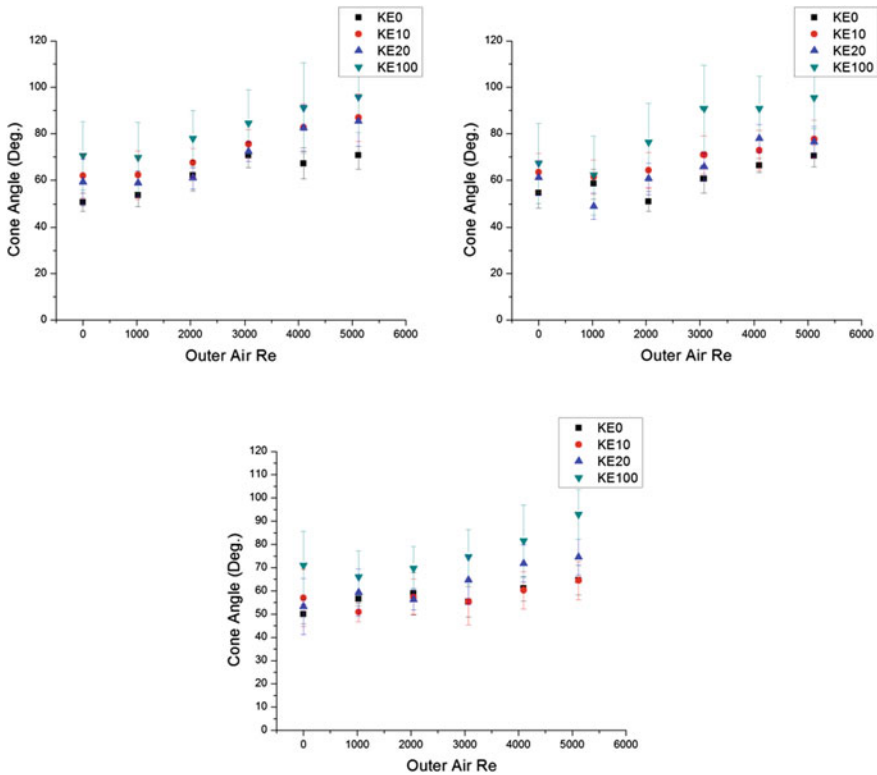

Fig. 9.18 Cone angle variation for different blended fuels with increasing inner air for outer co-swirl configuration and inner co-swirl (upper left), inner counter-swirl (upper right), and inner axial (below) configurations at 1 LPM fuel flow rate

The tulip shape is formed when the inner and outer flow rates are higher those that in case of onion shape as shown in Fig. 9.4d. The collapse of this bulge can be observed at some distance (along the axis) downstream. This occurs when no further expansion of the liquid sheet is allowed by the outer air. This distance is mostly found to decrease with increase in outer air flow rates. It can be observed from Fig. 9.4d that the outer periphery of the tulip-shaped spray is curved in nature unlike the conical shape observed for full cone spray as shown in Fig. 9.4e.

Figure 9.4e shows the spray regime known as the full cone-type spray. As shown in the figure, this regime has a conical shape at the outer periphery. An increase in the inner and outer air flow rates from that of the tulip spray regime results in a shorter breakup length. The breakup happens at a point closer to the nozzle outlet, and very short liquid sheet is present at the outlet of the nozzle leading to the formation of the full cone spray.

The early breakup regime as shown in Fig. 9.4f is formed at even high inner and outer air flow rates than those required for the formation of the full cone spray regime. The high swirling causes a high tangential velocity and creates a
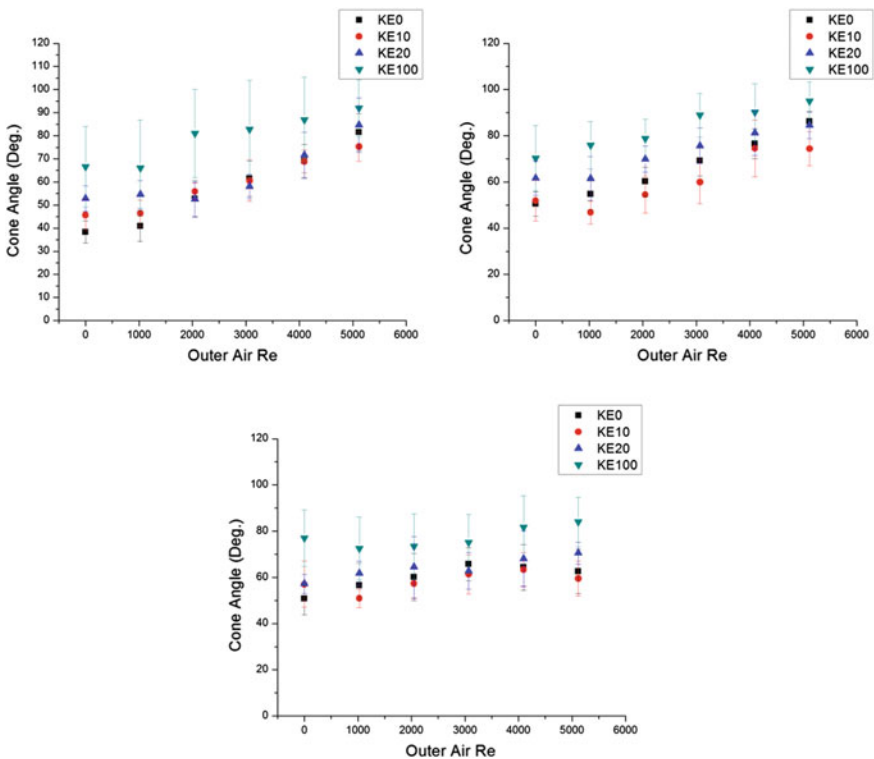

Fig. 9.19 Cone angle variation for different blended fuels with increasing inner air for outer counter-swirl configuration and inner co-swirl (upper left), inner counter-swirl (upper right), and inner axial (below) configurations at 1 LPM fuel flow rate

low-pressure regime outside the nozzle. The liquid sheet breaks at a point closer to the nozzle outlet creating a mist-type spray.

The early breakup regime and full cone-type spray are almost similar to each other. They only differ by the fact that the full cone-type spray shape has a small liquid sheet at the nozzle exit, whereas for the early breakup stage, this sheet breaks up very close to the nozzle exit.

Figure 9.5 shows the different breakup regime plots for 1 LPM kerosene flow for different inner and outer air flow rates and different flow configurations. Increase in the Weber number denotes the increase in air flow rate. At inner axial configuration, the early breakup stage shows up at high outer and inner air flow. However, for the inner co-swirl and counter-swirl configurations, early breakup stage occurs at high inner air flow and low outer air flow rate. Inner air flow and outer air flow play an important role in the formation of different spray breakup stages. Big onion-type shape is not present at inner axial flow condition. Onion-type, tulip-type, and full cone-type stages start to occur with increase in outer air flow at zero inner
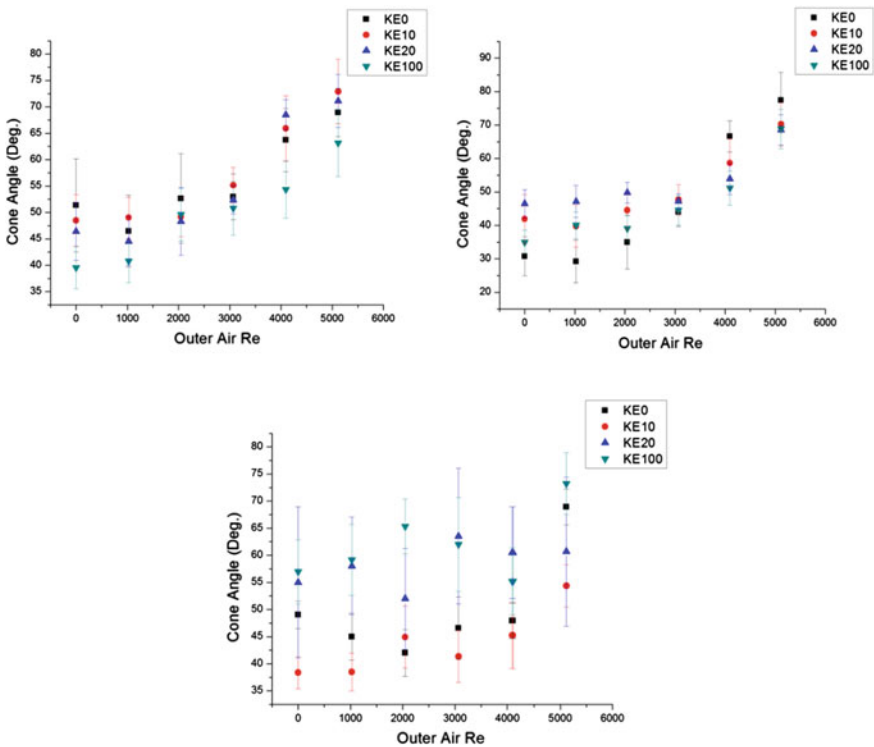

Fig. 9.20 Cone angle variation for different blended fuels with increasing inner air for outer co-swirl configuration and inner co-swirl (upper left), inner counter-swirl (upper right), and inner axial (below) configurations at 2 LPM fuel flow rate

air Weber number. Necklace-type shape is formed at lower inner and outer air Weber number.

Figure 9.6 shows the different breakup regime plots for 2 LPM kerosene flow for different inner and outer air flow rates and different flow configurations. It can be observed that the early breakup regime is not present in the inner and outer air co-swirl configurations; however, for other inner and outer air swirl configurations, early breakup regime is present. Full cone-type spray shape happens quickly in inner axial configuration than that in inner air swirl configuration at low outer air Weber number and 70 inner air Weber number. Big onion-type spray regime is present in more air flow configurations on inner counter-swirl and outer co-swirl configurations.

Figure 9.7 shows the different breakup regime plots for 1 LPM ethanol flow for different inner and outer air flow rates and different air flow configurations. Big onion-type breakup regime is not found for the ethanol 1 LPM flow. Early breakup regime arises quickly in inner air swirling configuration. At high inner and outer air flow conditions, early breakup regimes are present in all types of air flow configurations. Onion-type spray regime and full cone spray regime are not present in outer counter-swirl configuration at zero inner air Weber number.
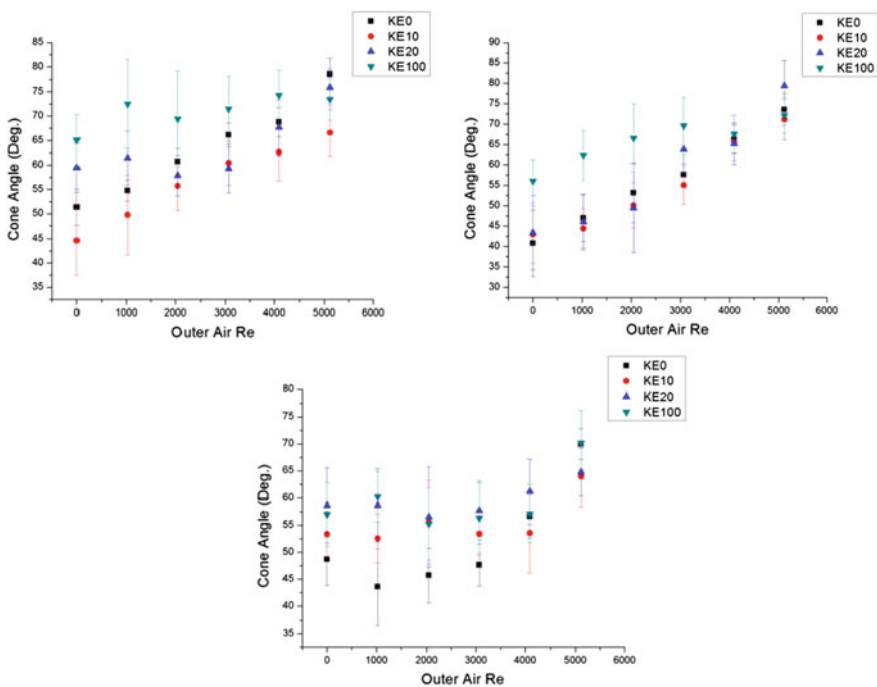

Fig. 9.21 Cone angle variation for different blended fuels with increasing inner air for outer counter-swirl configuration and inner co-swirl (upper left), inner counter-swirl (upper right), and inner axial (below) configurations at 2 LPM fuel flow rate

Figure 9.8 shows the different breakup regime plots for 2 LPM ethanol flow for different inner and outer air flow rates and different air flow configurations. Big onion-type regime is present in inner axial configuration and zero Weber number for outer counter-swirl configuration. The difference between tulip and full cone regime is almost negligible. Similarly, a trivial difference is present between the full cone and early breakup regimes. Early breakup regime is present at high inner and outer air flow conditions for all air flow configurations without inner co-swirl and outer co-swirl configurations. Necklace-type breakup regime is not present in inner co-swirl and outer co-swirl configurations.

Figure 9.9 shows the different breakup regime plots for 1 LPM 10% ethanol-blended kerosene flow for different inner and outer air flow rates and different air flow configurations. Big onion-type breakup regime formation is not found in 10% ethanol-blended kerosene fuel for 1 LPM fuel flow rate. At zero inner air Weber number with increasing outer air Weber number, the onion-type breakup phase is not present in any air flow configuration. The development of the spray phase is very rapid from the jet-type breakup regime to tulip-type breakup regime at
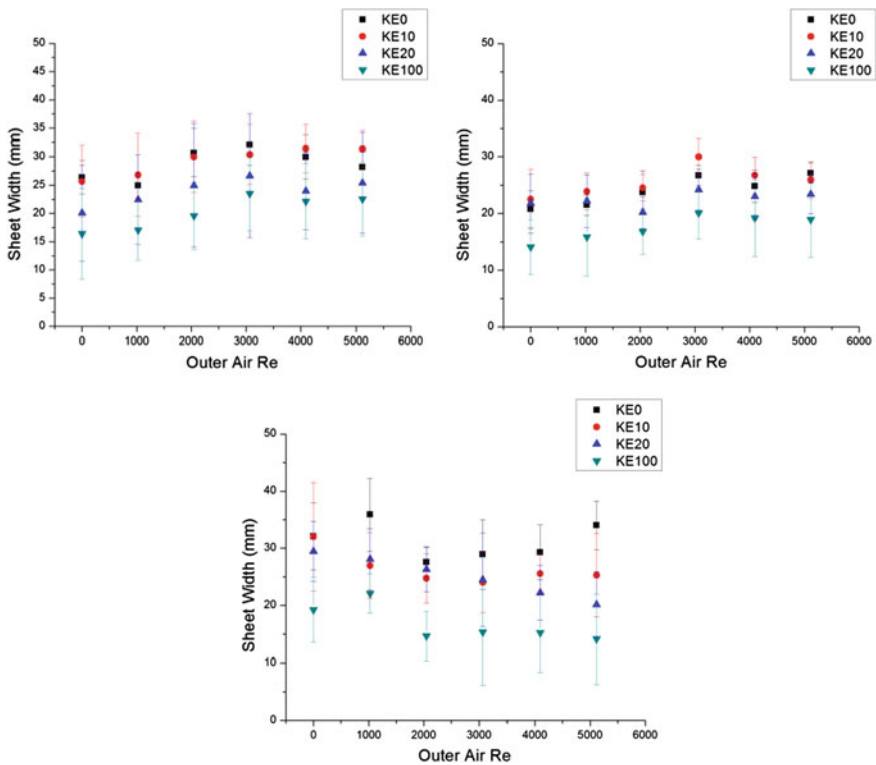

Fig. 9.22 Sheet width variation for different blended fuels with increasing inner air for outer co-swirl configuration and inner co-swirl (upper left), inner counter-swirl (upper right), and inner axial (below) configurations at 1 LPM fuel flow rate

zero inner air Weber number with increasing outer air Weber number. Early breakup regime is found at high inner air flow and outer air flow.

Figure 9.10 shows the different breakup regime plots for 2 LPM 10% ethanol-blended kerosene flow for different inner and outer air flow rates and different air flow configurations. In this case, the nature of the breakup regime is almost similar to that of other fuel regime plots.

Figures 9.11 and 9.12 show the different breakup regime plots for 1 LPM and 2 LPM 20% ethanol-blended kerosene flow, respectively, for different inner and outer air flow rates and different air flow configurations. The nature of the breakup regimes is similar to that of regimes observed earlier. The effect of variation in fuel properties does not seem to have much effect on the formation of the spray breakup regimes. The reason for this unusual behavior may be attributed to the fact that the properties like viscosity and surface tension differ very slightly for kerosene, ethanol, and ethanol-blended fuels.

The spray regimes depend on the swirling configuration and the fuel property only up to a certain degree. However, they are mainly dependent on the flow
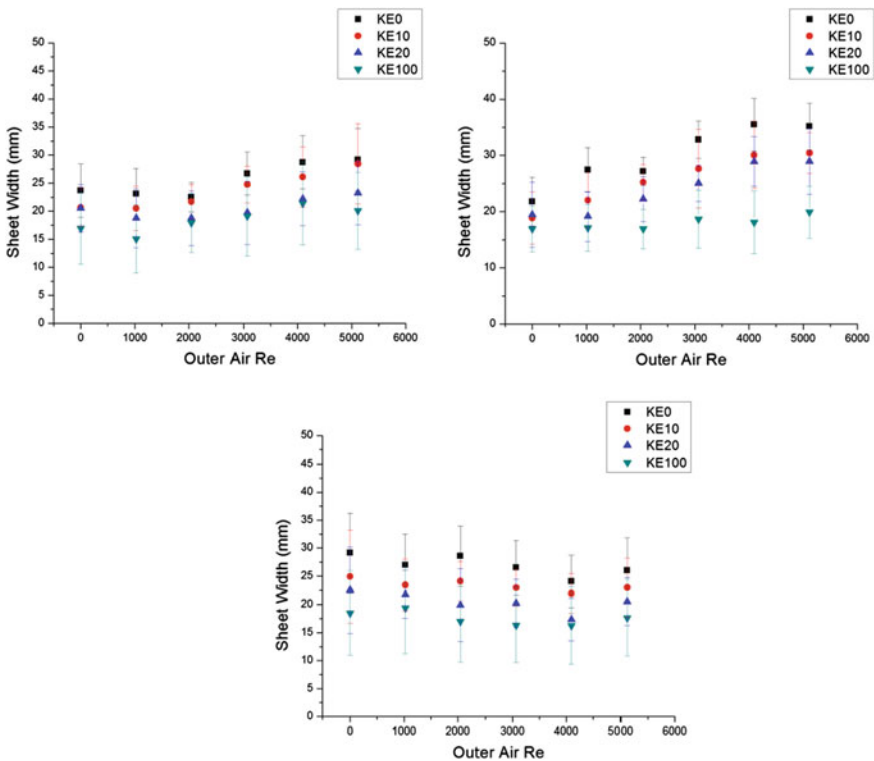

Fig. 9.23 Sheet width variation for different blended fuels with increasing inner air for outer counter-swirl configuration and inner co-swirl (upper left), inner counter-swirl (upper right), and inner axial (below) configurations at 1 LPM fuel flow rate

velocity. At low inner and outer air flow rates, initially, the jet flow regime appears. Upon increasing both the air flow rates, the necklace-type and onion-type regimes follow. Upon further increasing the air flow rates, tulip-type, full cone-type, and early breakup-type spray regimes are formed.

9.3.2 Macroscopic Spray Characteristics

Macroscopic spray characteristics of the spray are mainly breakup length, sheet width, and cone angle. Breakup of liquid sheets occurs when a discontinuity is observed. A continuous sheet gives rise to droplets and ligaments at the point of breakup. The breakup length is defined as the axial distance between the outlet of the nozzle and the sheet breakup point. Cone angle is measured by calculating the angle between the two lines made by the spray cone in the images obtained from high-speed camera. Sheet width is the maximum width of the liquid fuel sheet before breakup occurs. For this macroscopic measurement, inner air 20 LPM flow
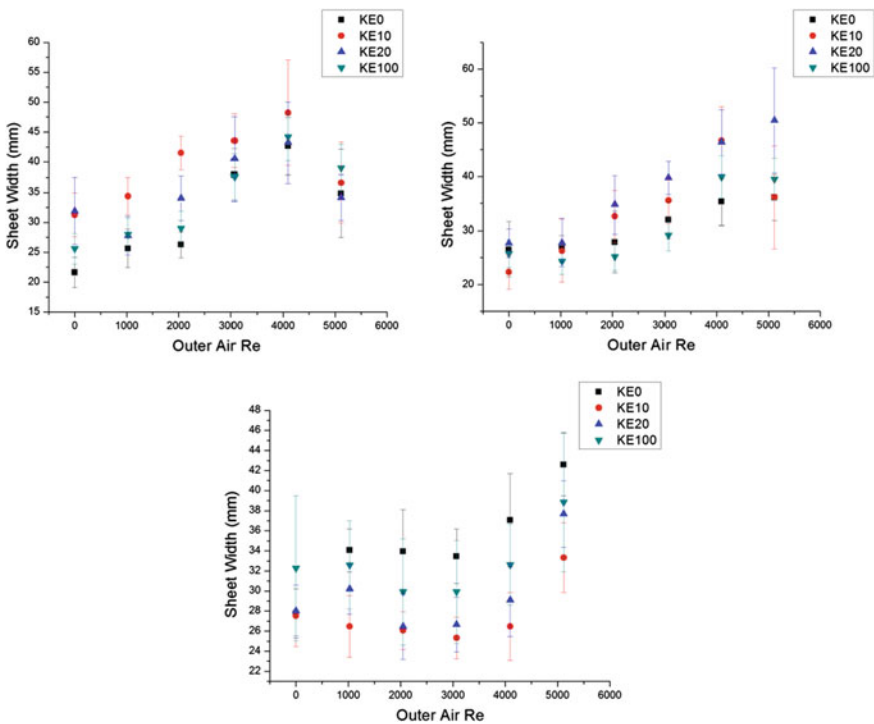

Fig. 9.24 Sheet width variation for different blended fuels with increasing inner air for outer co-swirl configuration and inner co-swirl (upper left), inner counter-swirl (upper right), and inner axial (below) configurations at 2 LPM fuel flow rate

rate is considered. At 30 LPM inner air flow, maximum spray belongs to early break-type spray phase. Primary breakup length measurement in early breakup stage is not so easy. Lower than 20 LPM inner air flow, the spray structure is not developed. For comparing the macroscopic spray characteristics for different fuels, the tests are done on 20 LPM inner air flow condition with 0–50 LPM outer air flow condition. Figure 9.13 shows the macroscopic spray characteristics measurement technique.

Figure 9.14 shows the breakup length variation for different blended fuels with increasing outer air flow at 1 LPM liquid flow for outer co-swirl configuration with inner axial, co-swirl, and counter-swirl configurations. At low air flow, breakup length variation is more in inner co-swirl and outer co-swirling configurations for all used fuels. But for inner axial configuration, the breakup length variation is more at intermediate outer air flow. At high air flow rate, the breakup length is almost similar for kerosene, kerosene-blended fuel, and ethanol. In outer co-swirl and inner counter-swirl configurations, the breakup length variation is very small for different used fuels.

Figure 9.15 shows the breakup length variation for different blended fuels with increasing outer air flow at 1 LPM liquid flow for outer counter-swirl configuration
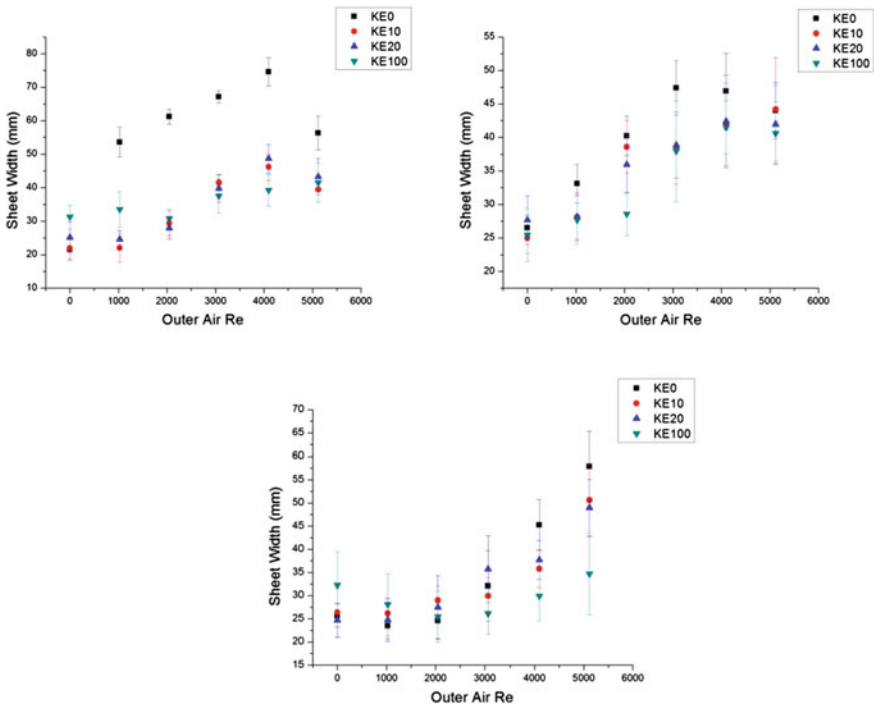

Fig. 9.25 Sheet width variation for different blended fuels with increasing inner air for outer counter-swirl configuration and inner co-swirl (upper left), inner counter-swirl (upper right), and inner axial (below) configurations at 2 LPM fuel flow rate

with inner axial, co-swirl, and counter-swirl configurations. Inner counter outer counter swirling configuration ethanol breakup length is minimum when compared to other used fuels, but in inner axial configuration, kerosene breakup length is maximum among all cases. Ethanol breakup is minimum in every configuration due to lower viscosity and surface tension. Kerosene, ethanol and ethanol blended kerosene fuel surface tension and viscosity difference is quite low, due to this reason the breakup length variation is small. Ethanol (KE100) breakup is small for almost every configuration than other used fuels.

Figure 9.16 shows the breakup length variation for different blended fuels with increasing outer air flow at 2 LPM liquid flow for outer co-swirl configuration with inner axial, co-swirl, and counter-swirl configurations. At 2 LPM liquid flow ethanol, breakup length is small, compared to that of other fuel breakup lengths. The breakup length pattern is almost similar to diesel and ethanol-blended diesel 2 LPM pattern. Figure 9.17 shows the breakup variation for outer counter-swirl configuration for 2 LPM fuel flow rate. With increasing blend percentages, the breakup length decreases in almost every condition. Ethanol (KE100) breakup length is minimum than other blended fuels. Kerosene and ethanol-blended kerosene breakup lengths are almost same but only in inner co and outer counter-swirl configuration kerosene breakup length is more than ethanol-blended kerosene at low outer air flow rate but at high outer flow condition breakup length variation is less for kerosene and ethanol blended kerosene fuel.

Figure 9.18 shows the outer air co-swirling effect at 1LPM liquid flow on kerosene, ethanol, and ethanol-blended kerosene. Here, the ethanol cone angle is maximum compared to kerosene and ethanol-blended kerosene fuel. The cone angle increases with increasing outer air flow rate. Cone angle increasing nature with outer air flow represents that the spray divergence increases with increasing outer air flow rate.

The cone angle trend is the same for outer air counter-swirl configuration (Fig. 9.19). The viscosity effect is prominent. For this reason, ethanol cone angle is more than corresponding cases of kerosene and ethanol-blended kerosene. But, Kerosene and ethanol blended kerosene have very close values of viscosity and surface tension. Hence, the cone angle variation is less. The variation of cone angle on inner air axial configuration for both outer air configurations is less for used fuel with increasing outer air flow than inner air co-swirl and counter-swirl configurations due to the inner air axial velocity.

Figures 9.20 and 9.21 show the outer air co-swirl and counter-swirl effect and inner air co-swirl and counter-swirl and axial direction effect on cone angle at 2 LPM air flow rate. Cone angle increases with increasing outer air flow. Viscosity difference in kerosene, ethanol, and ethanol-blended kerosene is very low. This may be the reason for differences in cone angle pattern with other cases. But the ethanol cone angle is more than kerosene and ethanol-blended kerosene fuel on outer counter-swirl configuration. The viscosity effect is not so prominent in this cone angle with outer air plot.

Figures 9.22 and 9.23 show the effect of outer air co-swirl and counter-swirl for three inner air flow configurations on sheet width at 1 LPM fuel flow. Here, the

kerosene sheet width is the highest and ethanol sheet width is the lowest for every flow condition. The blends lie between the kerosene and ethanol sheet widths. Here, with increasing blend percentage, the sheet width is decreasing. Kerosene and 10% ethanol- blended kerosene sheet width is almost same for outer air co and inner air co and counter swirl configurations as concluded from the experimental data.

Figures 9.24 and 9.25 show the effect of outer air co-swirl and counter-swirl for three inner air flow configurations on sheet width at 2 LPM fuel flow. For this condition, the plot does not follow any discernible pattern. Ethanol and kerosene and ethanol-blended kerosene do not have a high difference in viscosity and surface tension. May be for this reason the nature of the plot is very random. In inner co-swirl for both outer co-swirl and counter-swirl configuration, the nature of the plot is almost the same for all used fuels; sheet width increases with increasing outer air flow at low outer air flow rates, and then suddenly, sheet width decreases with increasing outer air flow.

9.4 Conclusions

The motivation behind the present experimental study is to ascertain the spray characteristics of kerosene, ethanol, and ethanol-blended kerosene. Different breakup phases are studied during this study. The breakup phases are very much dependent on the inlet flow velocity. The phases are less dependent on the viscosity and surface tension of the fuels used. With increasing inner and outer air flow rates, the breakup regime develops accordingly, from jet-type breakup regime to fully developed spray regime.

The present experiments have also been done for understanding the macroscopic behavior of spray for kerosene, ethanol, and ethanol-blended kerosene. A comparative study is done for different blended fuels with the conventional fuel. For this experimental investigation, we used a hybrid atomizer for determining the inner and outer air effect on the swirling annular liquid sheet. From the results of the current study, we broadly conclude that with increasing percentage of ethanol in blended fuels, the breakup length decreases and the cone angle increases. Ethanol-blended diesel and kerosene fuel spray characteristics are almost similar to conventional fuel. But on increasing blend percentage, the spray characteristics were found to be better than those of conventional fuel. Inner air axial configuration for both outer air swirl conditions, the spray characteristics is different compared to the inner air swirl configuration.

References

Ajav EA, Akingbehin OA (2002) A study of some fuel properties of local ethanol blended with diesel fuel. Agric Eng Int CIGR J Sci Res Dev IV:1–9

Chatterjee S et al (2013) Effect of Co and counter-swirling inner air on the spray dynamics of an annular fuel sheet in a hybrid atomizer. In: Ninth Asia-Pacific conference on combustion, The Combustion Institute (Korean section), Paper 2013-129, Pittsburgh, PA

Carvalho IS, Heitor MV (1998a) Liquid film break-up in a model of a prefilming airblast nozzle. Exp Fluids 1998(24):408–415

Carvalho IS, Heitor MV (1998b) Liquid film break-up in a model of a prefilming airblast nozzle. Exp Fluids 24(5):408–415

Chatterjee S et al (2014) Effect of geometric variations on the spray dynamics of an annular fuel sheet in a hybrid atomizer. Atomization Sprays 24(8):673–694

Chatterjee S et al (2015) Experimental investigation of breakup of annular liquid sheet in a hybrid atomizer. J Propul Power 2015(31):1232–1241

Chen H, Shi-Jin S, Jian-Xin W (2007) Study on combustion characteristics and PM emission of diesel engines using ester–ethanol–diesel blended fuels. Proc Combust Inst 31(2):2981–2989

Chiariello F et al (2014) Gaseous and particulate emissions of a micro gas turbine fueled by straight vegetable oil–kerosene blends. Exp Thermal Fluid Sci 56(july):16–22

Chin JS, Rizk NK, Razdan MK (1999) Study on hybrid airblast atomization. J Propul Power 15 (2):241–247

Chin JS, Rizk NK, Razdan MK (1999b) Study on hybrid airblast atomization. J Propul Power 15 (2):241–247

Dioha IJ et al (2012) Comparative studies of ethanol and kerosene fuels and cook stoves performance. J Nat Sci Res 2(6). http://www.iiste.org

Duke D, Honnery D, Soria J (2010) A cross-correlation velocimetry technique for breakup of an annular liquid sheet. Exp Fluids 49(2):435–445

Garai A et al (2017) Experimental investigation of spray characteristics of kerosene and ethanol-blended kerosene using a gas turbine hybrid atomizer. Sadhana 42(7):543–555

Hansen AC, Zhang Q, Lyne PWL (2005) Ethanol–diesel fuel blends—a review. Biores Technol 96(3):277–285

He B-Q et al (2003) The effect of ethanol blended diesel fuels on emissions from a diesel engine. Atmos Environ 37(35):4965–4971

Ibrahim AA, Jog MA (2007) Nonlinear breakup model for a liquid sheet emanating from a pressure-swirl atomizer. J Eng Gas Turbines Power 129(4):945–953

Khalil AEE, Gupta AK (2013) Fuel flexible distributed combustion for efficient and clean gas turbine engines. Appl Energy 109:267–274

Khan MY, Khan FA, Beg MS (2013) Ethanol-kerosene blends: fuel option for kerosene wick stove. Int J Eng Res Appl (IJERA) 3(1):464–466

Lapuerta M, Armas O, García-Contreras R (2007) Stability of diesel–bioethanol blends for use in diesel engines. Fuel 2007(86):1351–1357

Leboucher N, Roger F, Carreau J-L (2010) Disintegration process of an annular liquid sheet assisted by coaxial gaseous coflow(s) 20(10):847–862

Lefebvre AH (1989) Atomization and sprays. Hemisphere Publishing Corporation

Li D-G et al (2005) Physico-chemical properties of ethanol–diesel blend fuel and its effect on performance and emissions of diesel engines. Renew Energy 30(6):967–976

Lin SP (2003) Breakup of liquid sheets and jets. Cambridge University Press

Ma Z (2002) Investigation on the internal flow characteristics of pressure swirl atomizers. University of Cincinnati

Mendez CJ, Parthasarathy RN, Gollahalli SR (2012) Performance and emission characteristics of a small scale gas turbine engine fueled with ethanol/jet A blends. In: 50th aerospace sciences meeting, AIAA, Nashville, Tennessee 2012. AIAAA, p 0522

Mendez CJ, Parthasarathy RN, Gollahalli SR (2014) Performance and emission characteristics of butanol/Jet A blends in a gas turbine engine. Appl Energy 118:135–140

Patra J et al (2015) Studies of combustion characteristics of kerosene ethanol blends in an axi-symmetric combustor. Fuel 144:205–213

Reeser LG, Acra APL, Lee T (1995) Covering solar energy into liquid fuels. Resource engineering & technology for a sustainable world, vol 2(1). ASAE, pp 8–11

Rizk NK, Chin JS, Razdan MK (1996) Influence of design configuration on hybrid atomizer performance. AIAA 1996. Paper 96-2628

Rizk NK, Chin JS, Razdan MK (1996) Influence of design configuration on hybrid atomizer performance. In: 32nd joint propulsion conference and exhibit. American Institute of Aeronautics and Astronautics

Sayin C (2010) Engine performance and exhaust gas emissions of methanol and ethanol–diesel blends. Fuel 2010(89):3410–3415

Vesztergom (2014) M.Z.U.T.V.F.p.w.w.b.S. Determination of viscosity with Ostwald viscometer. http://foundation01.chem.elte.hu/Chemistry_BSc_English_Group/BLOCK_08/Viscosity_2014BSc1_eng.pdf

Wahono S et al (2008) High-speed visualisation of primary break-up of an annular liquid sheet. Exp Fluids 2008(44):451–459

Xing-Cai L et al (2004) Effect of cetane number improver on heat release rate and emissions of high speed diesel engine fueled with ethanol–diesel blend fuel. Fuel 83(14–15):2013–2020

Yahya RK, Goering CE (1977) Some trends in fifty-five years of Nebraska tractor test data. ASAE paper no MC-77-503, 1977. ASAE, St. Joseph, Ml 49085

Zhao H et al (2015) Breakup morphology of annular liquid sheet with an inner round air stream. Chem Eng Sci 137:412–422